Journal of Rajasthan Academy of Physical Sciences
ISSN : 0972-6306; URL : http://raops.org.in
Vol.15, No.1&2, March-June, 2016, 1-18

ENTROPY ANALYSIS FOR MHD CASSON FLUID FLOW IN A CHANNEL SUBJECTED TO WEAKLY TEMPERATURE DEPENDENT CONVECTION COEFFICIENT AND HYDRODYNAMIC SLIP

Paresh Vyas and Swati Soni
Department of Mathematics, University of Rajasthan, Jaipur-302004, India
E-mail: pvyasmaths@gmail.com, swatisoni19@yahoo.in

Abstract: Entropy generation analysis for steady MHD Couette Casson dissipative fluid flow in a channel is considered. The channel of width H is consists of uniformly moving impermeable plate and a stationary naturally permeable base. The upper plate bears a constant temperature while the base is subjected to convective flux with weakly temperature dependent convection coefficient and hydrodynamic slip. A uniform magnetic field is applied transversely to the flow direction. The non dimensionalised momentum and energy equations have closed form solution respectively which are used to compute entropy generation rate. The effects of pertinent parameters on the system are investigated through graphs and discussed.

Key Words: Entropy analysis, Casson fluid, MHD, hydrodynamic slip, convective flux

1. Introduction

Convective flow inside channels subjected to variety of end conditions serve as good baby models to large scale analogues complex real world system simply because such idealized flow geometries do appear as a single unit or in conjunction with other configurations. It was Berman [4] who presented first classical paper on laminar flow between two porous parallel plates. Recently, Tsangaris et al.[37] referred to a series of studies about the flow through porous channel/tubes of Newtonian and non Newtonian fluids.

Studying heat transfer in non-Newtonian fluid flow inside channels is worth for practical points of view. Flow inside parallel plate channel is often investigated simply because it provides initial estimates for complex flow configurations such as journal bearing etc. Many investigators have conducted some pertinent relevant studies. Lin [26] examined plane Couette flow and heat transfer for non- Newtonian fluids. Sukhow et al. [36] examined heat transfer to non- Newtonian fluid flow inside a parallel plate channel. Cotta

and Ozisik [10] examined laminar forced convection to non- Newtonian fluids in ducts with prescribed heat flux. Etemad et al.[13] investigated viscous dissipation effects in entrance region heat transfer for a power law fluid flowing between parallel plates. Tso et al.[38] investigated viscous dissipation effect of power law fluid flow inside parallel plate channel with constant heat fluxes. Pinho et al.[33] conducted analysis of forced convection in pipes and channels with the simplified Phan-Thien-Tanner fluid. Coehlo et al. [9] examined fully developed forced convection of the Phan-Thien-Tanner fluid in ducts with a constant wall temperature. Hashemabdi et al. [17,18] investigated forced convection heat transfer of Couette-Poiseuille flow of non-linear viscoelastic fluid between parallel plates. Raisi et al.[34] provided an approximate solution for the Couette-Poiseuille flow of the Gieskuis model between parallel plates. Khatibi et al.[24] reported forced convection heat transfer of viscoelastic fluid in pipes and channels. Flow and thermal characteristics in channels involving porous medium are worth studying since these find applications in many realms such as heat exchangers, chemical reactors, geothermal mechanisms etc. Many authors have reported pertinent studies on flow in channels involving porous medium. Chauhan and Vyas [6] investigated heat transfer in Couette flow of compressible fluid in naturally permeable channel. Vyas and Srivastava[39] studied radiation effects on MHD Couette flow in a composite channel. Vyas and Srivastava [40] also examined radiative MHD Couette flow of compressible fluid in a channel with permeable base.

The works reported above and the references contained therein and other relevant works not reported here have focussed on heat transfer aspects of non-Newtonian fluids flowing in channels. The majority previous studies in such flow configurations have been focussed on first law of thermodynamics only. The second law of thermodynamics is still a relatively low explored area.

An entropy analysis is pertinent for non Newtonian fluid flow and heat transfer in channels. The flow configurations owing to ample technological application such as solid matrix, heat exchangers, thermal insulation, electronic components cooling etc must be treated for inherent thermodynamic irreversibility in order to devise optimal system. The entropy optimization help practicing engineers to design thermal systems with lesser energy losses and consequently maximum possible energy available for use. Bejan [2,3] demonstrated that devices involving convective regime can be optimized by performing entropy generation analysis. He emphasized that the first and second laws of thermodynamics are global in nature and it is the second law (and the skill of the designer employing it) which has key to optimal thermal device through identifying the parameters responsible for entropy generation.He emphasized that the combined heat transfer and thermodynamics model “portrays” irreversible nature of the device and thus the optimization of such a model gives us a feel for the other abstract concept of entropy generation, specifically where and how much of it is being generated, how it flows, and how it impacts thermodynamic performance. Entropy analysis has proved to be a pertinent technique to help thermodynamic optimization emerge as a self-standing research area. Last two decades have witnessed upsurge of entropy analysis in convective regimes.

Last two decades have witnessed a great surge of activity in entropy generation analysis and entropy generation minimization enabling these emerge as self sustained research discipline to form a basis for good engineering design. Erbay et al. [12] computed entropy generation during fluid flow between parallel plates with moving bottom. In series of papers, Mahmud and Fraser [28,30] flow and thermal characteristics inside channels/pipe. Many authors have reported entropy analysis in channels filled with porous medium or permeable walls [5, 7, 8, 11, 16, 19, 20, 21, 22, 23, 27, 29, 31, 32, 41, 42, 44, 45]. Here it is worth to make a point here that none of the study reported above or elsewhere and the references contained there in considered the setup as taken in this study. In this paper, we have considered MHD Couette flow and heat transfer inside a channel with permeable bottom subjected to hydrodynamic slip and thermal condition of third kind where convective coefficient is weakly temperature dependent. The thermal behaviour of the flow inside the channel strongly depends on the end conditions. The thermal boundary conditions of third kind i.e. Fourier-Newton's law of cooling means that the amount of heat entering or leaving the system depends on the ambient temperature T_a^* and the effective convective heat transfer coefficient (which includes thermal wall resistance and the external convective heat transfer coefficient). Further, the effective convective heat transfer coefficient is presumed to be weakly temperature dependent. The hydrodynamic slip at the permeable bottom is accounted by Saffman conditions [35]. Here, we wish to recall that when slug flow over a porous medium takes place, then the flow inside the porous medium is governed by the Darcy law. However, it is worth to note that in the absence of any pressure gradient and for small permeability, the interior flow of the porous medium would not contribute much to the exterior clean fluid flow and therefore zero "filter velocity" in the permeable bed may be assumed. However the permeability of the permeable bed affects the clean fluid flow through the microscopic boundary condition as suggested by Saffman [35] who modified the Beavers- Joseph condition [1] by applying a statistical approach and ensemble averaging to strongly non- homogeneous porous media. He showed that for small permeability, they following equation is appropriate to compute the exterior clean fluid correct to $o(K_0^*)$,

$$u^* = \left(\frac{\sqrt{K_0^*}}{\alpha}\right)\left(\frac{du^*}{dy^*}\right) + o(K_0^*)$$

Where y* refers to the direction normal to the boundary, u* is the tangential fluid velocity, K* is the permeability and α is the dimensionless empirical constant depending upon the material parameters characterizing the structure of the porous material. Beavers-Joseph [1] found that the slip coefficient α demonstrated the values 0.78,1.45 and 4.0 for foam metal having average pore size 0.016,0.034 and 0.045 inches respectively. It is emphasised that α has nothing to do with fluid viscosity but has dependence on flow direction at the interface, Reynolds number, the extent of the clean fluid and known uniformities in the arrangements of solid material at the permeable surface. Here it is worth to note that various values of α have been determined empirically without compromising the permeability or bulk porosity of the porous medium. This enables us to

use α as possible parameter in comfiguration involving porous medium. In the ensuing text we have shown its effect on quantities of interest.

Many theoretical models on convective flux with uniform convection coefficient have been reported in literature. Idealization of a uniform heat transfer coefficient is not always realistic since in certain applications, the heat transfer may change with the local temperature in non linear fashion. In particular, the cooling process may follow power law type temperature dependence or weakly temperature dependence. It has been empirically found that the heat convection mechanism is mostly temperature dependent. Many authors have reported studies on temperature dependent convection mechanism in different realms [14,15,25]. An intense survey of literature revealed that most of the works on entropy generation analysis for convective flux problems have considered uniform heat transfer coefficient. This prompted us to carry out entropy analysis taking temperature dependent convection mechanism so as to realise realistic model and fill the void. Further, it is emphasised that the configuration considered here has not been addressed though it is an interesting situation to look into for it is expected that the presented model would serve as pertinent introductory model to large scale analogous simulations.

2. Formulation of the problem

We consider the steady fully developed dissipative flow of a viscous incompressible Casson fluid in a parallel plate channel of width H with a stationary naturally permeable base. The upper wall of the channel moves with a uniform velocity.

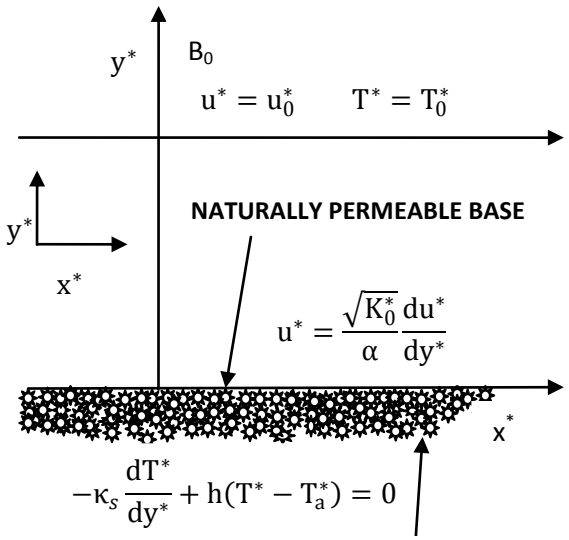

Fig. 1. Coordinates and Flow configuration

A Cartesian coordinate system (x^*, y^*, z^*) is assumed such that the x*-axis coincides with the surface of the stationary permeable base and y^*-axis normal to it (Fig. 1). Let $V = (u^*,v^*,w^*)$ be the velocity vector. It is further assumed that the velocity and temperature fields are hydrodynamically and thermally fully developed in the channel, and for such flow situation, we have unidirectional flow in the x^*-direction between channel walls at $y^* = H$ and $y^* = 0$ This unidirectional flow implies that $v^* = w^* = 0$. Let the width of the channel walls parallel to the z^*-axis be large compared to the distance between the channel walls. Thus, all the variables are independent of z^*.

Further with the help of continuity equation, we have $\frac{\partial u^*}{\partial x^*} = 0$ and thus conclude that the only nonzero velocity component u^* will be a function of y^* alone.

A transverse magnetic field of strength B_0 is applied. The upper impermeable wall of the channel located at $y^* = H$ moves with uniform velocity u_0^* and is maintained at uniform temperature T_0^* whereas the lower stationary naturally permeable wall at $y^* = 0$ experiences convective flux and hydrodynamic slip. The convection coefficient is presumed to be weakly temperature dependent. We neglect the induced magnetic field, under the assumption, that the magnetic Reynolds number is small. For some practical engineering problem, it is an important case, where the conductivity is not large, but the strength of the magnetic field is large. Further, in the absence of an externally applied electric field and with negligible effects of polarization voltages, we also assume that $E = 0$. The flow in the channel is driven by the shear generated due to the motion of the upper wall only. The flow is fully developed hydrodynamically and thermally, hence the fluid velocity $u^*$and the temperature T^*in the channel are functions of y^* only.

The rheological equation of state for an isotropic and incompressible flow of a Casson fluid is

$$\tau_{ij} = \begin{cases} 2\,(\mu_B + p_y/\sqrt{2\pi})e_{ij}\,, & \pi > \pi_c \\ 2\,(\mu_B + p_y/\sqrt{2\pi_c})e_{ij}, & \pi < \pi_c, \end{cases} \tag{1}$$

where $\pi = e_{ij}e_{ij}$, and e_{ij} is the (i, j)th component of deformation rate, π is the product of the component of deformation rate with itself, π_c is a critical value of this product based on the non-Newtonian model, μ_B is the plastic dynamic viscosity of non-Newtonian fluid, and p_y is the yield stress of fluid.

Thus, the governing equations for the set up described above are given as follows

$$\nu\left(1+\frac{1}{\beta}\right)\frac{d^2u^*}{dy^{*2}} - \frac{\sigma B_0^2 u^*}{\rho} = 0 \tag{2}$$

$$\frac{\kappa}{\rho c_p}\frac{d^2T^*}{dy^{*2}} + \frac{\sigma B_0^2 u^{*2}}{\rho c_p} + \frac{\nu}{c_p}\left(1+\frac{1}{\beta}\right)\left(\frac{du^*}{dy^*}\right)^2 = 0 \tag{3}$$

Together with the boundary conditions

$$y^* = 0;\ u^* = \frac{\sqrt{K_0^*}}{\alpha}\frac{du^*}{dy^*}\,, \qquad \kappa_s\frac{dT^*}{dy^*} + h(T^* - T_a^*) = 0$$

$$y^* = H; \qquad u^* = u_0^* \qquad T^* = T_0^* \tag{4}$$

Where $\nu = (\mu_B/\rho)$ is the kinematic viscosity, κ is thermal conductivity of the fluid, K_0^* is permeability, T_0^* is the temperature of the upper plate, σ is the electric conductivity, $\beta = \mu_B\, 2\pi_c/p_y$ is the Casson parameter, ρ is the density of fluid, c_p is specific heat at constant pressure, κ_s is the effective thermal conductivity of the permeable surface, T_a^* is ambient temperature, and h is weakly temperature dependent convection coefficient as follows :

$$h = h_a\left\{1 + \frac{\varepsilon(T^* - T_a^*)}{T_0^* - T_a^*}\right\} \tag{5}$$

where h_a is reference convection coefficient and ε is small linearity coefficient.

We introduce the following non-dimensional quantities

$$u = \frac{u^*}{u_0^*}, \quad \eta = \frac{y^*}{H}, \quad \theta = \frac{T^* - T_a^*}{T_0^* - T_a^*}, \quad K = \frac{K_0^*}{H^2} \tag{6}$$

Using equations (5) and (6), the equations (2) and (3) take the following respective non-dimensional forms

$$\frac{d^2u}{d\eta^2} - \frac{M^2}{1+\frac{1}{\beta}}u = 0 \tag{7}$$

$$\frac{d^2\theta}{d\eta^2} + Br\left[M^2u^2 + \left(1+\frac{1}{\beta}\right)\left(\frac{du}{d\eta}\right)^2\right] = 0 \tag{8}$$

And the boundary conditions (4),in non-dimensional form become

$$\eta = 0: \quad u = \frac{\sqrt{K}}{\alpha}\frac{du}{d\eta}, \qquad \frac{d\theta}{d\eta} = -Bi(1+\varepsilon\theta)\theta$$

$$\eta = 0: \quad u = 1, \quad \theta = 1 \tag{9}$$

Where,

$$M = \sqrt{\frac{\sigma B_0^2 H^2}{\rho}}, \quad Br = \frac{\mu_B u_0^{*2}}{\kappa(T_0^* - T_a^*)}, \quad Bi = \frac{h_a H}{\kappa_s}$$

are Hartmann number, Brinkman number and Biot number respectively.

Solution

The boundary value problem described by equations (6) through (8) provides closed form analytical solutions for velocity and temperature, and we have velocity u and temperature θ as follows

$$\mathbf{u = C_1 e^{\frac{M\eta}{\sqrt{1+\frac{1}{\beta}}}} + C_2 e^{\frac{-M\eta}{\sqrt{1+\frac{1}{\beta}}}}} \tag{10}$$

$$\theta = \frac{-Br\left(1+\frac{1}{\beta}\right)}{2}\left(C_1{}^2 e^{\frac{2M\eta}{\sqrt{1+\frac{1}{\beta}}}} + C_2{}^2 e^{\frac{-2M\eta}{\sqrt{1+\frac{1}{\beta}}}}\right) + d_1\eta + d_2 \tag{11}$$

Where the constants of integration C_1, C_2 ,d_1, d_2 are computed in view of boundary conditions (9) and are obtained as follows:

$$C_1 = \frac{M + \alpha\sqrt{\frac{1+\frac{1}{\beta}}{K}}}{e^{\frac{M}{\sqrt{1+\frac{1}{\beta}}}}\left(M + \alpha\sqrt{\frac{1+\frac{1}{\beta}}{K}}\right) + e^{\frac{-M}{\sqrt{1+\frac{1}{\beta}}}}\left(M - \alpha\sqrt{\frac{1+\frac{1}{\beta}}{K}}\right)}$$

$$C_2 = \frac{M - \alpha\sqrt{\frac{1+\frac{1}{\beta}}{K}}}{e^{\frac{M}{\sqrt{1+\frac{1}{\beta}}}}\left(M + \alpha\sqrt{\frac{1+\frac{1}{\beta}}{K}}\right) + e^{\frac{-M}{\sqrt{1+\frac{1}{\beta}}}}\left(M - \alpha\sqrt{\frac{1+\frac{1}{\beta}}{K}}\right)}$$

$$d_2 = C_1' + \frac{(1-Bi) - \sqrt{(Bi-1)^2 + 4Bi\varepsilon\left(C_1' + C_2'\right)}}{2Bi\varepsilon},$$

$$C_1' = \frac{Br\left(1+\frac{1}{\beta}\right)}{2}\left({C_1}^2 + {C_2}^2\right),$$

$$C_2' = MBr\sqrt{1+\frac{1}{\beta}}\left({C_1}^2 - {C_2}^2\right) - 1 - \frac{Br\left(1+\frac{1}{\beta}\right)}{2}\left({C_1}^2 e^{\frac{2M}{\sqrt{1+\frac{1}{\beta}}}} + {C_2}^2 e^{\frac{-2M}{\sqrt{1+\frac{1}{\beta}}}}\right),$$

$$d_1 = C_3' - d_2,$$

$$C_3' = 1 + \frac{Br\left(1+\frac{1}{\beta}\right)}{2}\left({C_1}^2 e^{\frac{2M}{\sqrt{1+\frac{1}{\beta}}}} + {C_2}^2 e^{\frac{-2M}{\sqrt{1+\frac{1}{\beta}}}}\right)$$

3. Second law analysis

The local volumetric rate of entropy generation S_G for a viscous MHD fluid flow is defined as follows(Woods [43])

$$S_G = \frac{\kappa}{T_0^{*2}}\left(\frac{dT^*}{dy^*}\right)^2 + \frac{\mu_B\left(1+\frac{1}{\beta}\right)}{T_0^*}\left(\frac{du^*}{dy^*}\right)^2 + \frac{\sigma B_0^2 u^{*2}}{T_0^*}$$

$$S_G = \frac{\kappa}{H^2}\frac{(T_0^* - T_a^*)^2}{T_0^{*2}}\left(\frac{d\theta}{d\eta}\right)^2 + \frac{\mu_B u_0^*\left(1+\frac{1}{\beta}\right)}{H^2 T_0^*}\left(\frac{du}{d\eta}\right)^2 + \frac{\sigma B_0^2 u_0^* u^2}{T_0^*} \quad (12)$$

The first term on the R.H.S.of equation (12) is the local entropy generation due to heat transfer, the second term is the local entropy generation due to viscous dissipation with Casson parameter and the third term is the local entropy generation due to the effect of magnetic field. The velocity and temperature fields are utilized to compute entropy.

We introduce,

$$S_{G_0} = \frac{\kappa}{H^2}\frac{(T_0^* - T_a^*)^2}{T_0^{*2}} = (\text{charateristic entropy generation rate})$$

$$\omega = \frac{T_0^*}{T_0^* - T_a^*} = (\text{charateristic temperature ratio})$$

Thus the non-dimensional entropy generation N_s is obtained as follows:

$$N_s = \frac{S_G}{S_{G_0}} = \left(\frac{d\theta}{d\eta}\right)^2 + Br\omega\left[\left(1+\frac{1}{\beta}\right)\left(\frac{du}{d\eta}\right)^2 + M^2u^2\right] \;=\; HTI + FFI$$

where

$$HTI = \left(\frac{d\theta}{d\eta}\right)^2$$

is the heat transfer irreverisibility and

$$FFI = Br\omega\left[\left(1+\frac{1}{\beta}\right)\left(\frac{du}{d\eta}\right)^2 + M^2u^2\right]$$

is the dissipative irreversibility.

Further, Bejan number which is pertinent irreversibility measure is defined as

$$Be = \frac{HTI}{HTI + FFI}$$

In fact, *Be* = 0 represents the case when there is no irreversibility due to heat transfer hence only dissipations are responsible for irreversibility. And *Be* = 1 stands for the situation when heat transfer irreversibility dominates over fluid friction irreversibility such that there is no irreversibility due to dissipations. For the situations when Bejan number *Be* < 0.5, it means that fluid friction irreversibility is more dominant over irreversibility due to heat transfer.

This physical understanding helps decipher the figures.

4. Results and Discussions

We restrict our analysis to entropy generation only. The profiles for velocity and temperature have been drawn though not reported here for the sake of brevity. These profiles help decipher the entropy profiles.

Figures 2-9 display entropy generation variations and figures 10-17 display Bejan number variation respectively for various values of parameters. The figures depicting

entropy show that entropy is large in regions adjacent to channel walls and attains its minima “somewhere in the middle” of the channel. This may be attributed to the fact that the temperature attains peaks (vanishing temperature gradient) at different spatial distances η in the channel for respective values of set of parameters. Thus, one may conclude that in some part of the channel there is lesser heat transfer irreversibility due to vanishing temperature gradients. Further, it is seen that the entropy at the permeable wall where a non-vanishing velocity gradient and a convective flux is in force, is larger than that of at the impermeable wall. The Fig-2 depicts that entropy generation number N_s rises with increasing values of Hartmann number M. This goes well with the expectations since the increasing values of Hartmann number indicate stronger Lorentz force retarding the flow and giving rise to larger Ohmic dissipation (due to the term M^2u^2 present in energy equation (8) and entropy generation number equation (13). Figure-3 depicts that the entropy generation number N_s rises with the increasing values of slip coefficient α. We wish to emphasize that materials having same permeability or same bulk porosity exihibits different values of α as reported in the literature. Thus entropy may be controlled by adjusting the values of α without compromising the permeability of the permeable base. Thus slip coefficient α can serve as a pertinent controlling parameter in thermal system of interest involving permeable strip without compromising the permeability or bulk porosity of the porous medium. Fig-4 reveals that entropy decays with increasing values of Casson parameter β. Fig -5 exhibits that entropy decreases with the increasing values of permeability K. It is worth to observe that how even small values of K have a significant effect on entropy. This finding is of utmost importance where one may conclude that even a finer permeable strip with low permeability, if geometrical constraints allow, can be employed in devices to control entropy generation. In Fig-6 Entropy N_s increases with increasing values of Brinkman number. The larger values of Br indicate larger frictional heating in the system. The present dissipative set up shows rise in entropy with increasing values of Br.

Fig-7 reveals that with the increasing values of Biot number Bi, the entropy increases in the region close to permeable surface where a convective flux is applied. However, the trend is reversed in the region close to upper wall. Here, it is pertinent to point out that in heat transfer problems, the Biot Number and the Nusselt number have the same group of physical parameters: h H/k, where H is a characteristic length scale, h is a heat transfer coefficient, and k is the thermal conductivity. The Nusselt Number is used to characterize the heat flux from a solid surface to a fluid. In that case, the thermal conductivity is for the fluid. Normally in engineering applications , one can find correlations for the Nusselt number in terms of other dimensionless parameters that characterize the flow environment near the surface of the plate. The Biot number is used to characterize the heat transfer resistance "inside" a solid body. The Biot number in a body relates conductive heat transfer within a body and the convective heat transfer on the surface of said body. In that case k is the thermal conductivity of the solid body, and h is the heat transfer coefficient that describes the heat transferred from the "surface of the solid body" to the surrounding fluid. The Biot Number can be viewed as the ratio of internal diffusion resistance to external convection resistance.

Fig-8 displays that with increasing values of characteristic temperature ratio the entropy rises. Fig -9 shows that there is qualitative effect of ε on entropy generation. We see that when ε is increased then there is considerable decay in entropy generation number.

As far as Bejan number plots are concerened, we see that every parameter has a visible effect on Bejan number variations. Since it is a ratio of HTI and (HTI +FFI), hence its plots present a fair picture of irrversibility' causes and effects. We see that the Bejan number is large adjacent to permeable wall where a hydrodynamic slip and heat flux is in force as compared to that at the upper moving isothermal wall. Further, we observe that Bejan number attains minima at different spatial distance in the channel for different respective parameter values. The region, in which Be> ½, indicates that heat transfer irreversibility is more dominant over that due to dissipative efffects. The Fig-10 displays the effect of Hartmann number M on Bejan number Be. We see that with increasing values of M Bejan number rises in large sections of the channel adjacent to channel walls except in some part in the middle of the channel (i.e. $\eta = 0.5$ to $\eta = 0.7$). In Fig-11 the same trend in Be is witessed for varying values of slip coeffcient α. Fig- 12 depicts that with an increase in values of Casson parameter β, the Be increases till the spatial distance $\eta = 0.7$, and beyond this the trend is reversed. The Fig-13 shows that Be rises with an increase in K till a spatial distance $\eta = 0.74$, and then the trend is reversed. Similarly fig-15 shows that with increasing values of Bi, the Bejan number rises till a certain spatial distance, and then the trend is reversed. Fig-16 depicts that Bejan number Be decays with increasing values of characteristic temerature ratio ω. The Fig-17 shows that Bejan number Be decays with an increase in ε.

5. Conclusions

The study analyzed entropy analysis of MHD Couette flow of a Casson inside a naturally permeable channel. The lower channel wall was subject to hydrodynamic slip and convective flux wherein the convection coefficient was considered to be weakly temperature dependent. The upper uniformly moving wall of the channel was isothermal. The momentum and the energy equations offered closed-form solutions, which were employed to compute entropy generation. The results portrayed graphically lead to following conclusions:

1. There is pronounced entropy generation at the walls. It is found that there is an increase in *N*s by increasing Hartmann number M, Brinkman number Br and slip coefficient α.
2. Entropy generation number Ns decreases throughout the channel with an increase in Casson parameter β, Permeability parameter K and perturbation parameter ε.
3. Entropy generation number N_S increases with the increasing values of Biot number Bi in the region close to permeable surface where a convective flux is applied. However, the trend is reversed in the region close to upper wall.
4. Profiles for Bejan number Be show that Be is larger at the channel walls and it vanishes at spatial distances (different spatial distances for different parameter values). It is attributed to the situation when temperature attains its maxima i.e. vanishing temperature gradients, hence irreversibility due to heat transfer is zero.

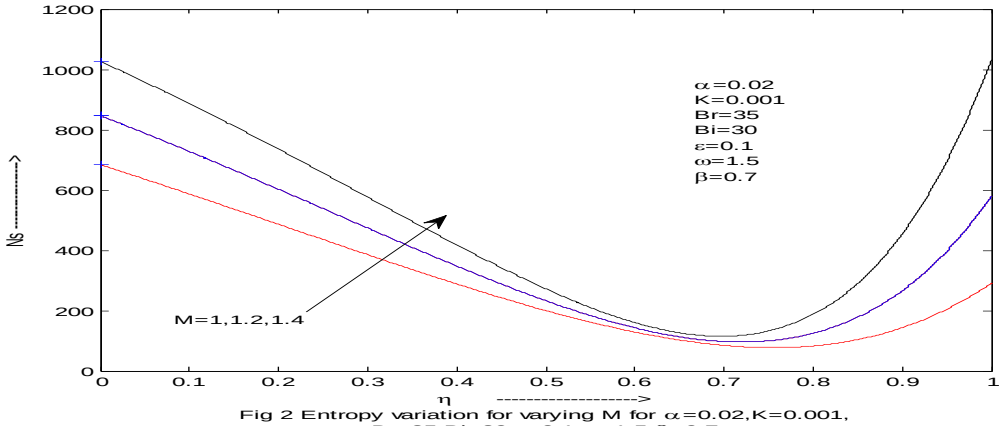

Fig 2 Entropy variation for varying M for α=0.02,K=0.001, Br=35,Bi=30,ε=0.1,ω=1.5,β=0.7

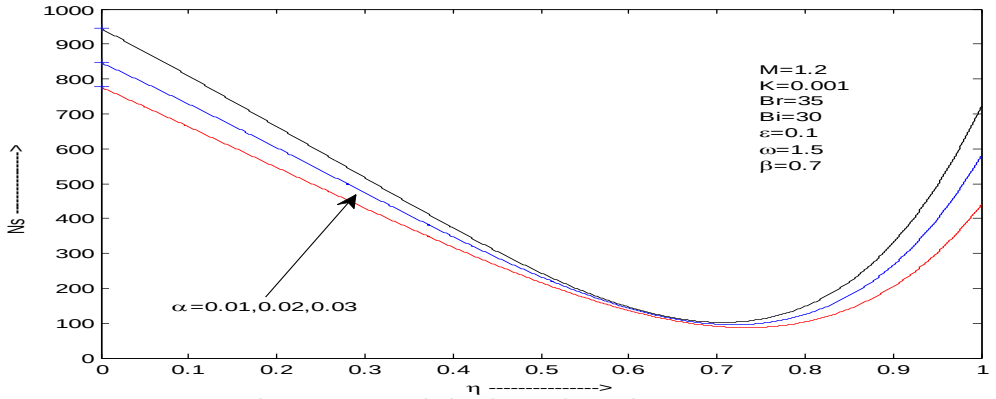

Fig 3 Entropy variation for varying α for M=1.2,K=0.001, Br=35,Bi=30,ε=0.1,ω=1.5,β=0.7

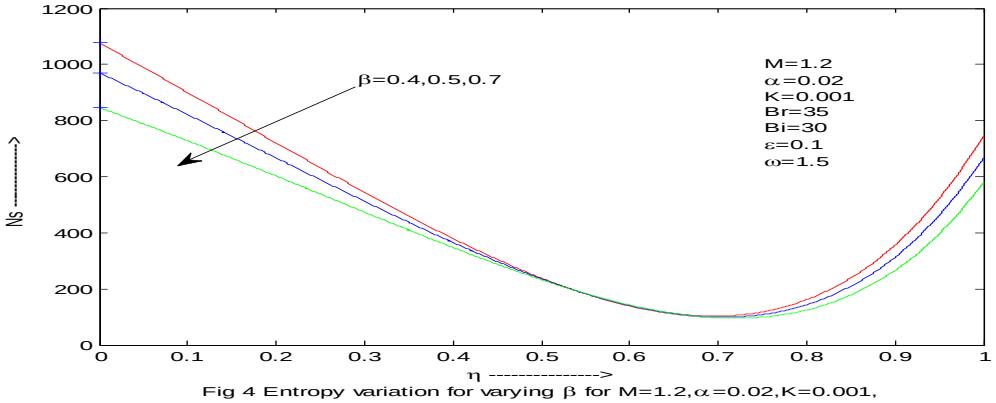

Fig 4 Entropy variation for varying β for M=1.2,α=0.02,K=0.001, Br=35,Bi=30,ε=0.1,ω=1.5

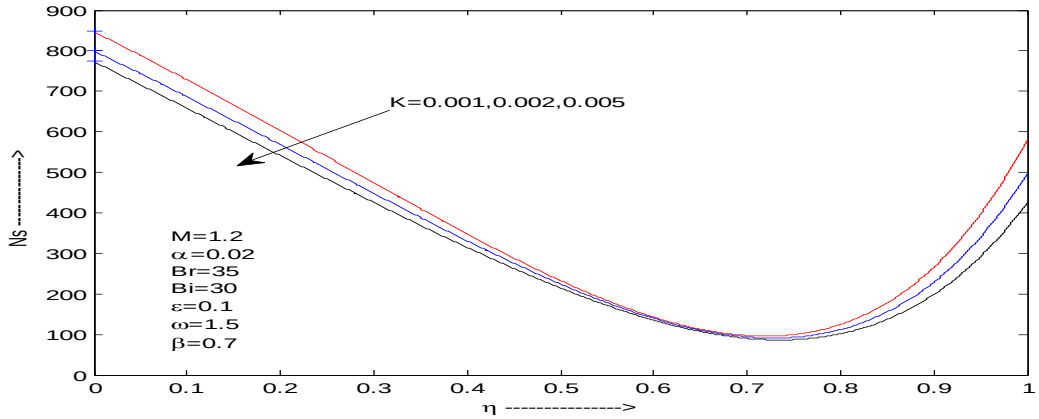

Fig 5 Entropy variation for varying K for M=1.2, α=0.02, Br=35, Bi=30, ε=0.1, ω=1.5, β=0.7

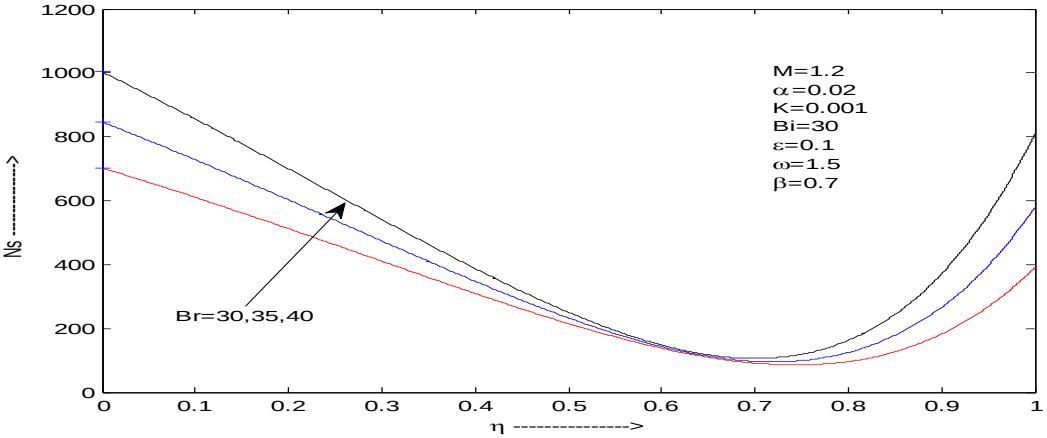

Fig 6 Entropy variation for varying Brinkmann Number for M=1.2, α=0.02, K=0.001, Bi=30, ε=0.1, ω=1.5, β=0.7

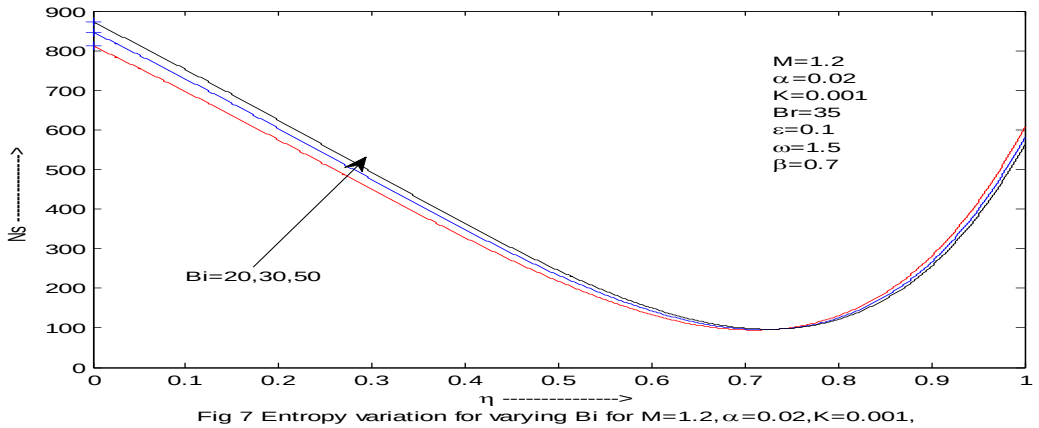

Fig 7 Entropy variation for varying Bi for M=1.2, α=0.02, K=0.001, Br=35, ε=0.1, ω=1.5, β=0.7

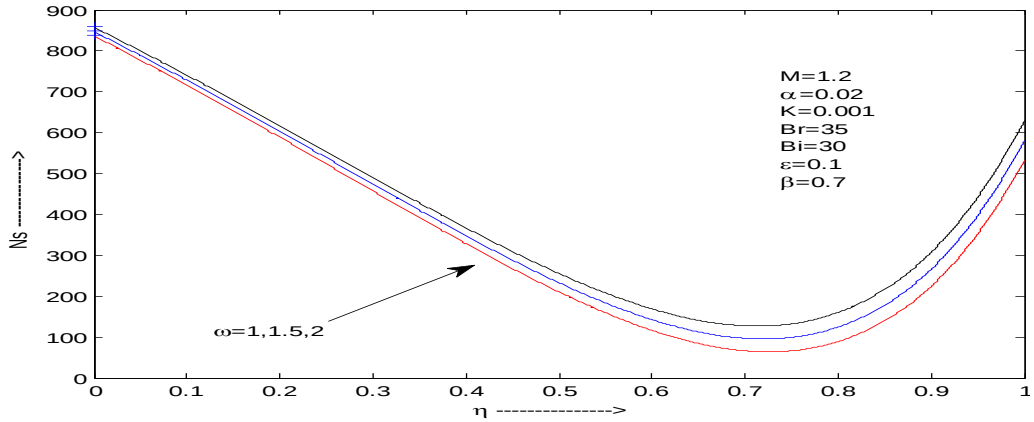

Fig 8 Entropy variation for varying ω for M=1.2,α=0.02, K=0.001,Br=35,Bi=30,ε=0.1,β=0.7

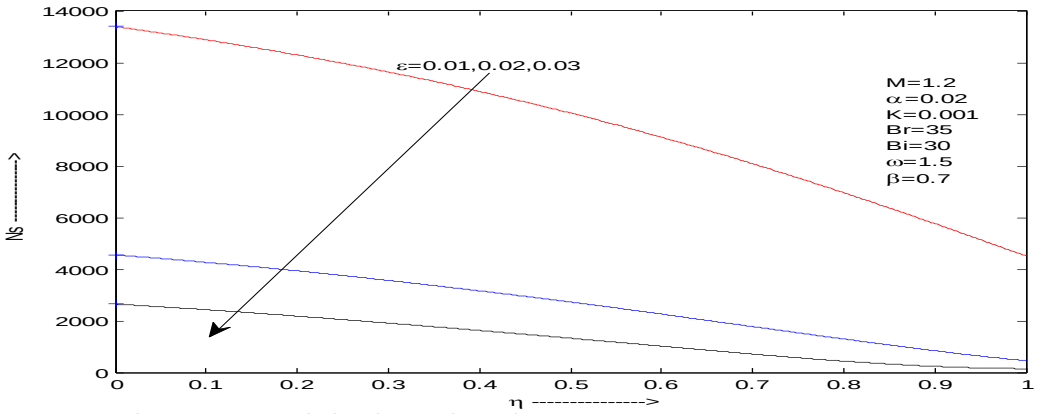

Fig 9 Entropy variation for varying ε for M=1.2,α=0.02, K=0.001,Br=35,Bi=30,ω=1.5,β=0.7

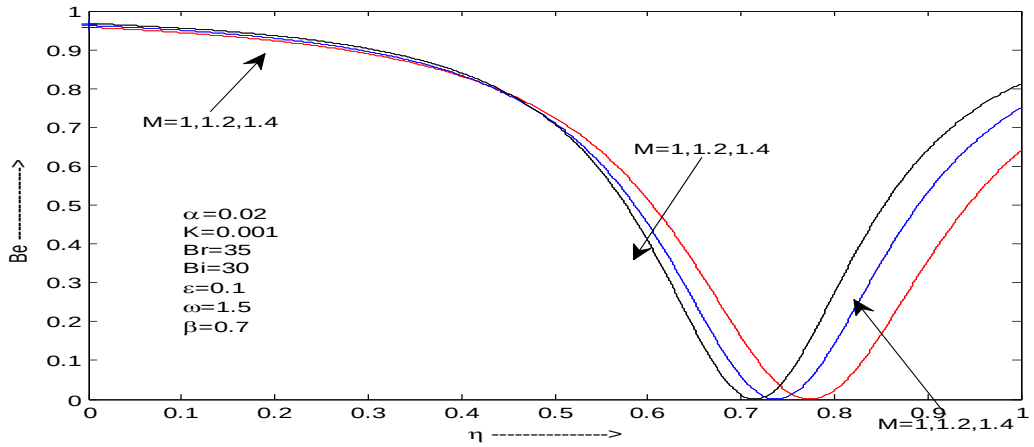

Fig 10 Bejan Number Variation for varying M for α=0.02,K=0.001, Br=35,Bi=30,ε=0.1,ω=1.5,β=0.7

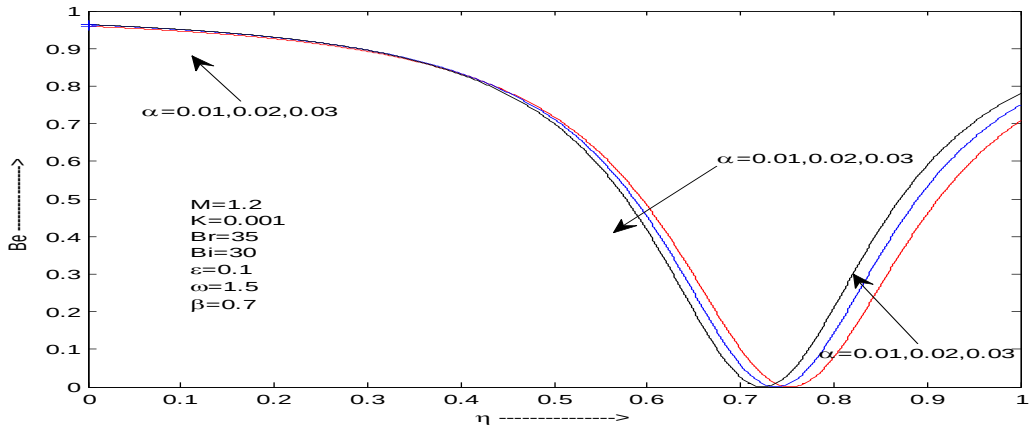

Fig 11 Bejan Number Variation for varying α for M=1.2,K=0.001, Br=35,Bi=30,ε=0.1,ω=1.5,β=0.7

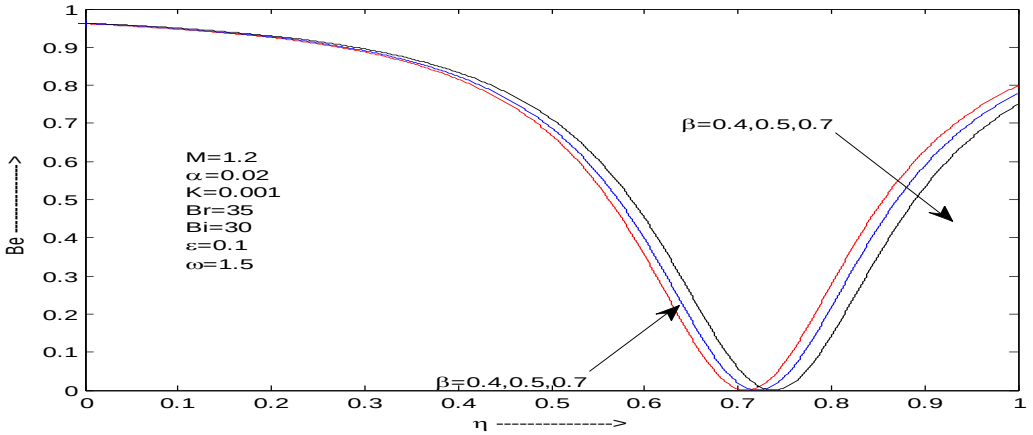

Fig 12 Bejan Number Variation for varying β for M=1.2,α=0.02,K=0.001, Br=35,Bi=30,ε=0.1,ω=1.5

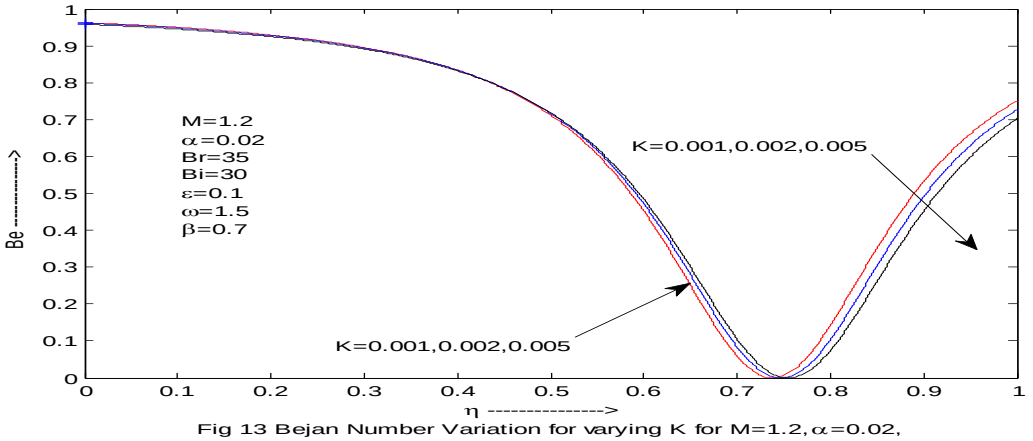

Fig 13 Bejan Number Variation for varying K for M=1.2,α=0.02, Br=35,Bi=30,ε=0.1,ω=1.5,β=0.7

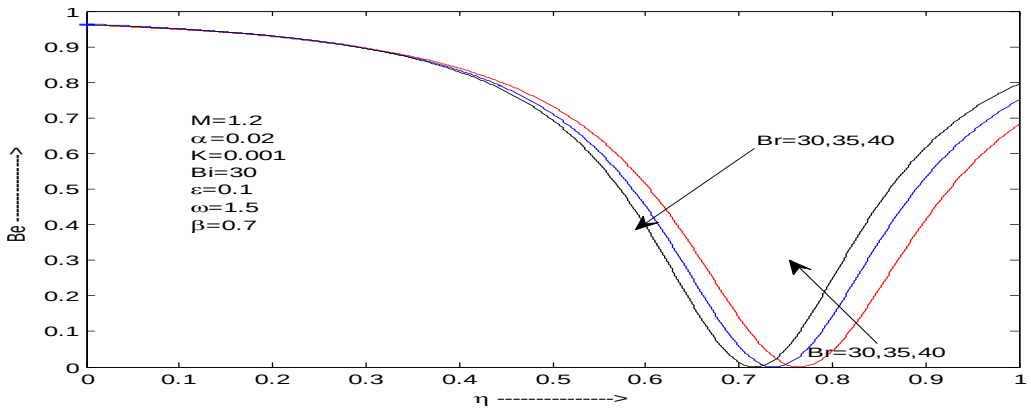

Fig 14 Bejan Number Variation for varying Brinkmann Number for M=1.2, α=0.02, K=0.001, Bi=30, ε=0.1, ω=1.5, β=0.7

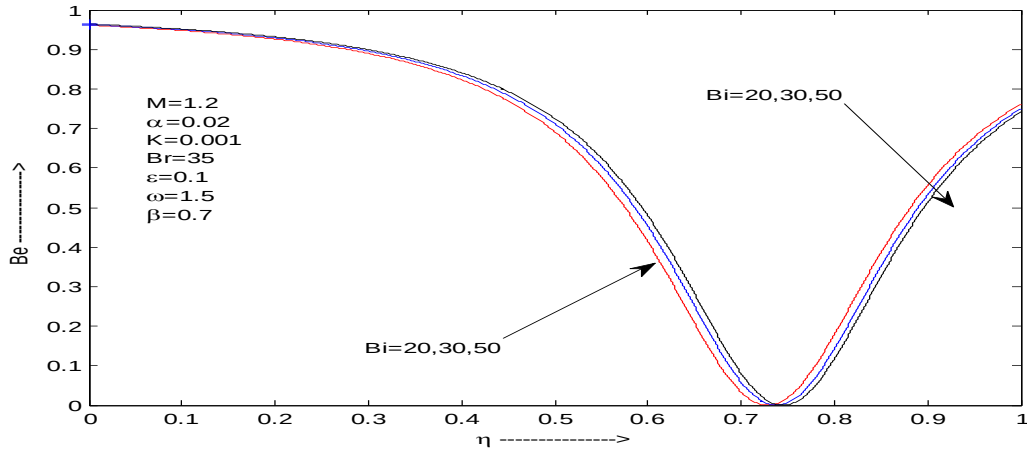

Fig 15 Bejan Number Variation for varying Bi for M=1.2, α=0.02, K=0.001, Br=35, ε=0.1, ω=1.5, β=0.7

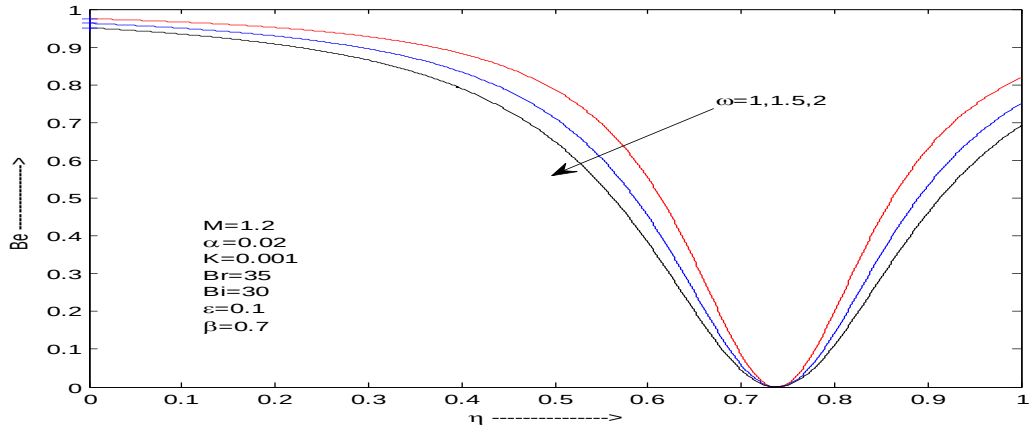

Fig 16 Bejan Number Variation for varying ω for M=1.2, α=0.02, K=0.001, Br=35, Bi=30, ε=0.1, β=0.7

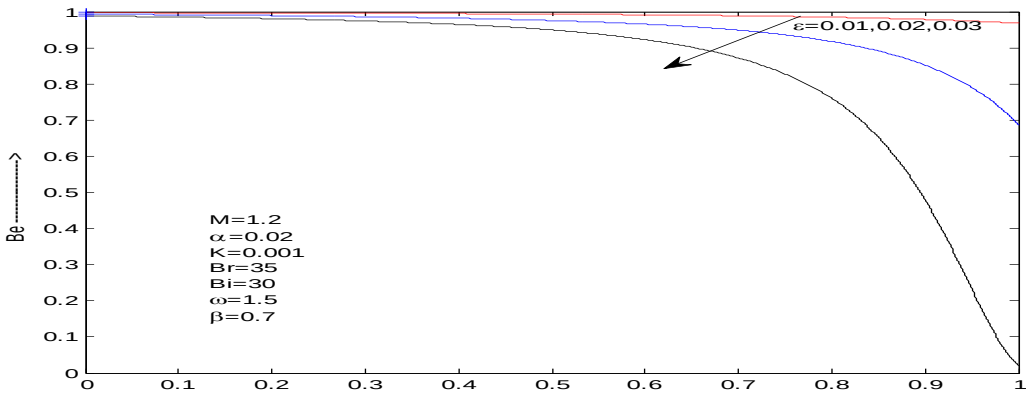

Fig 17 Bejan Number Variation for varying ε for M=1.2,α=0.02, K=0.001,Br=35,Bi=30,ω=1.5,β=0.7

References

[1] Beavers, G.S. and Joseph, D. D. (1967). Boundary conditions at a naturally permeable wall. *J. Fluid Mech.* 30, 197-207.

[2] Bejan, A. (1984). *Convection Heat Transfer*, Wiley, Hoboken.

[3] Bejan, A., Dincer, I., Lorente, S., Miguel, A.F., Reis, A.H. (2004). *Porous and Complex Flow Structures in Modern Technologies*, Springer, New York.

[4] Berman, A. S. (1953). Laminar Flow in Channels with Porous Walls, *J. Appl. Phys.* 24(9), 1232-1235.

[5] Chauhan, D.S. and Kumar, V. (2013). Entropy analysis for third grade fluid flow with temperature dependent viscosity in annulus partially filled with a porous medium, Theoret. *Appl. Mech.*, 40(3), 441–464.

[6] Chauhan, D.S. and Vyas, P. (1995). Heat Transfer in hydromagnetic Couette flow of compressible Newtonian fluid., *ASCE J. Eng. Mech.* 121, 57-61.

[7] Chen., Y. and Zhu, K. (2008). Couette- poisieille flow of bingham fluids between two porous parallel plates with slip conditions., *J. Non-Newtonian Fluid Mech.* 153, 1-11.

[8] Chinyoka , T. and Makinde , O.D. (2013). Analysis of entropy generation rate in an unsteady porous channel flow with Navier slip and convective cooling, *Entropy* 15, 2081-2099.

[9] Coelho, P. M., Pinho, F.T. and Oliveria, P. J. (2000). Fully developed forced convection of the Phan-Thien-Tanner fluid in ducts with a constant wall temperature ,*Int. J. Heat Mass Transfer* 45, 1413-1423.

[10] Cotta, R.M. and Ozisik, M.N. (1986). Laminar forced convection to non-Newtonian fluids in ducts with prescribed heat flux, *Int. Commun. Heat Mass Transfer* 13(3), 325-334.

[11] Eegunjobi, A.S. and Makinde, O.D. (2012). Effects of Navier slip on entropy generation in a porous channel with suction/injection, *J. Therm. Sci*. 7, 522-535.

[12] Erbay, L. B., Ercan, M. S., Sulus B. and Yalcin, M.M. (2003). Entropy generation during fluid flow between two parallel plates with moving bottom. *Entropy*, 5, 506-518.

[13] Etemad, S. G., Myumdar, A S. and Huang, B. (1994). Viscous dissipation effects in entrance region heat transfer for a power law fluid flowing between parallel plates, *Int. J. Heat Fluid Flow* 15(2), 122-131.

[14] Ghai, M.L. (1951). Heat transfer in straight fins, proceedings of general discussion on heat transfer, *Institute of Mechanical engineers, London*, p. 203-204.

[15] Ghai M. L. and Jakob, M. (1950). Local coefficients of heat transfer for straight fins, *Trans. ASME*, p. 1-21.

[16] Haddad, O., Abuzaid, M. and Al-Nimr, M. (2004), Entropy generation due to laminar incompressible forced convection flow through parallel plates micro channel., *Entropy* 6, 413-426.

[17] Hashemabadi, S. H., Etemad, S. G and Thibault, J. (2004). Forced convection heat transfer of Coutte-Poiseuille flow of non- linear viscoelastic fluids between parallel plates, *Int. J. Heat Mass Transfer* 47(2), 3985-39991.

[18] Hashemabadi, S. H., Etemad, S. G and Thibault, J. (2005). Analytical solution of viscoelastic fluid flow and heat transfer through an annulus, *Heat transfer Eng*. 26(2), 45-49.

[19] Hooman, K. and Ejlali, A. (2007). Entropy generation for forced convection in a porous saturated circular tube wiyh uniform wall temperature., *Int. Commn. Heat Mass transfer* 34,408-419.

[20] Ibanez G. and Cuevas, S. (2010), Entropy generation minimization of a MHD(Magneto hydrodynamics) flow in a microchannel. *Energy* 35, 4149-4156.

[21] Ibanez, G. (2015). Entropy generation in MHD porous channel with hydrodynamic slip and convective boundary conditions., *Int. J. Heat Mass Transfer* 80, 274-280.

[22] Ibanez, G., Lopez, A., Pantoja J. and Moreira, J. (2014). Combined effects of uniform heat flux boundary conditions and hydrodynamic slip on entropy generation in a microchannel. *Int. J. Heat Mass Transfer* 73, 201-206.

[23] Ibanez, G., Lopez, A., Pantoja J., Moreira, J. and Reyes, J.A. (2013). Optimum slip flow based on the minimization of entropy generation in parallel plate microchannels. *Energy* 50, 143-149.

[24] Khatibi, A. M., Mirzazadeh, M. and Rashidi F. (2010). Forced convection heat transfer of Giesekus viscoelastic fluid in pipes and channels, *Heat Mass Transfer*, 2010; 46(4), 405-412.

[25] Laor, K. and Kalman, H. (1996). Performance and optimum dimensions of different cooling fins with a temperature dependent heat transfer coefficient. *Int. J. Heat Mass Transfer* 39(9) , 1993-2003.

[26] Lin, S.H. (1979). Heat Transfer to plane Non-Newtonian Couette flow, *Int. J. Heat Mass Transfer* 22(7), 1117-1123.

[27] Lopez de Haro, M., Cuevas S. and Beltran, A. (2014). Heat transfer and entropy generation in the parallel plate flow of a power-law fluid with asymmetric convective cooling. *Energy* 66, 750-756.

[28] Mahmud, S. and Fraser, R.A. (2002). Thermodynamic analysis of flow and heat transfer inside channel with two parallel plates. *Energy* 2, 140-146.

[29] Mahmud, S. and Fraser, R.A. (2002). Inherent irreversibility of channel and pipe blows for Non- Newtonian fluids ,*Int. Commn. Heat Mass transfer* 29,.577-587.

[30] Mahmud, S. and Fraser, R.A. (2003). The second law analysis in fundamental convective heat transfer problems, *International journal of thermal sciences* 42, 177-186.

[31] Mahmud, S. and Fraser, R.A. (2005). Flow, thermal and Entropy generation characterises inside a porous channel with viscous dissipation . *Int. J. Thermal science* 44, 21-32.

[32] Makinde O.D. and Eegunjobi, A.S. (2013), Effects of convective heating on entropy generation rate in a channel with permeable walls, *Entropy* 15(1), 220-233.

[33] Pinho, F.T. and Oliveria, P. J. (2000). Analysis of forced convection in pipes and channels with the simplified Phan-Thien-Tanner fluid, *Int. J. Heat Mass Transfer* 43, 2273-2287.

[34] Raisi, A., Mirzazadeh, M., Dehnavi, A.S. and Rashidi. F. (2008). An approximate solution for the Couette- Poiseuille flow of the Giesekus model between parallel plates, *Rheol, Acta* 47(1), 75-80.

[35] Saffman, P. G. (1971). On the boundary condition at the surface of a porous medium, *Stud. Appl. Math*. 50, 93-101.

[36] Sukhow, W. H., Hrycak, P. and Griokey, R.G. (1980). Heat transfer to non-Newtonian dilatant (Shear-thickening) fluids flowing between parallel plates., *AICHE Symp*. 76(199) , 257-263.

[37] Tsangaris, S., Nikas, C., Tsangaris G. and Neofytou, P. (2007). Couette flow of a Bingham plastic in a channel with equality porous walls. *J. Non- Newtonian Fluid Mechanics* 144, 42-48.

[38] Tso, C.P., Shella-Francissa, J., Hung, Y.M. (2010). Viscous dissipation effects of power-law fluid flow within parallel plates with constant heat flues, *J. non-Newtonian Fluid Mech*. 165, 625-630.

[39] Vyas P. and Srivastava, N.(2013). Radiation effects on dissipative magenetohydro-dynamic Couette flow in a composite channel. *Z. Naturforsch* 68, 554-566.

[40] Vyas P. and Srivastava, N.(2014). Radiation MHD compressible couette flow in a parallel channel with a naturally permeable wall., *Therm. Sci,*. 18, (Suppl.2) S573-S585.

[41] Vyas P. and Srivastava, N.(2015). Entropy analysis of generalized MHD Couette flow inside a composite duct with asymmetric convective cooling., *Arabian J. for Science and Engineering* 40(2), 603-614.

[42] Vyas P. and Rai, A. (2013). Entropy regime for radiative MHD Coutte flow inside a channel with naturally permeable base., *Int. J. Energy Technol*. 5, 1-9.

[43] Woods, L.C. (1975). Thermodynamic of fluid Systems, *Oxford Uni. Press, Oxford* .

[44] Yazdi, M., Abdullah, S., Hashim I. and Sopian, K. (2013). Reducing entropy generation in MHD fluid flow over open parallel microchannels embedded in a micropatterned permeable surface, *Entropy* 15, 4822-4843.

[45] Yilbas, B.S., Yursoy M. and Pakdemerili, M. (2004). Entropy analysis for non Newtonian fluid flow in annular pipe : constant viscosity case. *Entropy*, 6,304-315.